Journal of Directed Energy, **1**, Spring 2004, 171–181

Conceptual Design of a High-Power, High-Gain Free-Electron Laser Amplifier

Dinh C. Nguyen,* Sergey S. Kurennoy, and Lloyd M. Young

Los Alamos National Laboratory, Los Alamos, New Mexico 87545

and

Henry P. Freund

Science Applications International Corporation, 1710 Goodridge Drive, McLean, Virginia 22102

High-gain free-electron laser (FEL) amplifiers offer unique advantages such as robust operation without a high-Q optical cavity and potentially high extraction efficiencies with the use of tapered wigglers. Although a high average power, continuous-wave FEL amplifier has not been demonstrated, many key physics issues such as electron beam brightness requirements, single-pass gain, saturation, etc., have been resolved. We study the feasibility of a high-power FEL based on the high-gain, combination-wiggler amplifier. We show that with suitable electron beam parameters, peak output power of 1 GW can be directly achieved. We also outline a possible configuration of a high-power, high-gain FEL amplifier with energy recovery.

KEYWORDS: Energy recovery, High-gain FEL amplifier, High-power FEL

1. Introduction

The free-electron laser (FEL) holds the promise of an all-electric, high-optical-quality, megawatt-power laser weapon that consumes only water and electricity, therefore requiring a simple logistical trail. The FEL produces a wavelength-adjustable output with flexible pulse formats to induce a range of effects on the targets from denial to destruction. A particular kind of FEL, the radio frequency (RF) linear accelerator (linac) FEL, offers high-quality electron beams for generating high-power and short-wavelength coherent light and adjustable output pulse formats that typically consist of a train of picosecond pulses separated by a multiple of the RF period. The individual picosecond pulses are called the micropulses, and a train of micropulses is called a macropulse (Fig. 1). The macropulses are adjustable from a few RF periods to several hours, depending on the duration of the high-power RF voltage that is applied to the RF linac for accelerating the electron beams. Macropulse power is a measure of the FEL capability to sustain a high level of performance at high electron beam current without beam breakup and at high optical power without optical damage. The highest macropulse power achieved thus far was 0.73 MW at 200 GHz during 10-μs macropulses.[9]

Received February 24, 2003; revision received June 27, 2003.

*Corresponding author; e-mail: dcnguyen@lanl.gov.

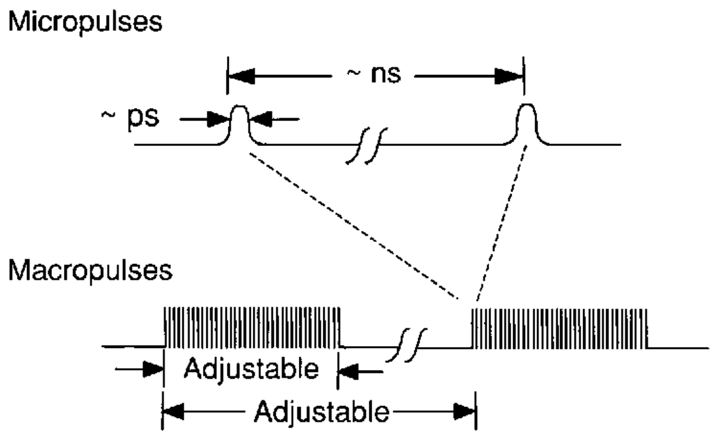

Fig. 1. Pulse format of a typical RF linac FEL.

Operating the FEL at shorter wavelengths thus far has produced lower macropulse power because of reduced FEL extraction efficiencies.[5,6] Efficiency improvement with a tapered wiggler is yet to be demonstrated at optical wavelengths. A nice feature with the FEL pulse format is the flexibility of "dialing" lethality effects, from denying to destruction, by controlling the FEL duty factor, by changing either the micropulse repetition rate or the macropulse duration.

The physics of FEL saturation sets the peak power during the micropulse in the range of a few hundred megawatts to a few gigawatts. This range is determined by the nominal electron beam parameters and the typical FEL extraction efficiency of a few percent. FEL saturation occurs when the electrons trapped in the ponderomotive potential rotate one-half of the synchrotron period and more than half of the electrons reside in the lower half of the bucket (Fig. 2), a situation analogous to the two-level laser. In an amplifier FEL, this entire saturated power is available to the users. In an oscillator configuration, the FEL output peak power is the intracavity saturated power times the out-coupling fraction of the partially reflecting mirror, typically a few percent depending on the single-pass gain. (The higher out-coupling fraction requires a larger single-pass gain.) Two important knobs for scaling the FEL average power are the micropulse energy, the product of output peak power and micropulse duration, and the micropulse repetition rate. Megawatt power can be achieved with the RF linac FEL by increasing either the micropulse energy or the micropulse repetition rate, or both. As an example, a megawatt FEL could produce 2 mJ of micropulse energy at a repetition rate of 500 MHz.

The superconducting RF linac FEL at the Jefferson Laboratory achieved a continuous-wave (cw) average power of 2.1 kW. Operating at 74.85 MHz, this oscillator FEL produced micropulse energy of 28 μJ, corresponding to 40-MW peak power during the 0.7-ps (full width at half-maximum; fwhm) micropulses.[5] A demonstration at Los Alamos of a high-gain, low-Q oscillator FEL concept called the regenerative amplifier FEL (RAFEL), where approximately 66% of the intracavity power was coupled to the outside, achieved micropulse energy of 1.3 mJ, corresponding to 80-MW peak power during the 16-ps (fwhm) micropulses. The higher micropulse energy was a result of a larger out-coupling fraction, higher extraction efficiency, and longer micropulse length. With a micropulse repetition rate of 108 MHz, the RAFEL achieved 140-kW power during the 15-μs macropulse.[6]

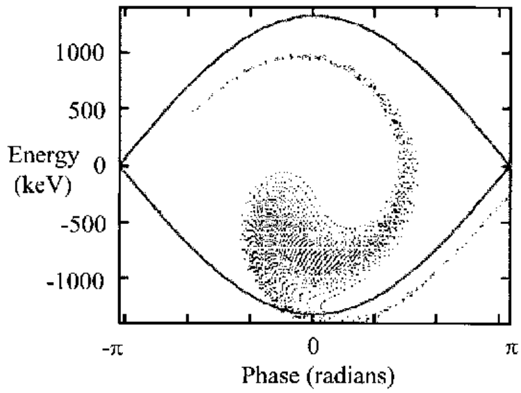

Fig. 2. FEL saturation in a uniform wiggler. The ponderomotive bucket is plotted over one wavelength along the horizontal axis. The vertical axis is in kiloelectron volts, and the bucket constitutes about ±2% of the original beam energy.

Although this experiment constituted the proof of concept of the RAFEL, the apparatus was not designed for high-duty operation. Since the macropulse duty factor, a fraction of time the macropulses were on, was only 10^{-4}, the RAFEL cw average power was only 14 W. Nevertheless, the RAFEL showed that important FEL physics such as steady-state performance at high peak power, optical damage, wakefields, etc., could be resolved over a few tens of microseconds, a timescale long enough for these effects to manifest themselves.

Two distinct RF linac technologies exist for powering the FEL: the low-duty, normal-conducting RF copper linac and the high-duty, superconducting RF (SRF) niobium linac. Owing to high RF surface ohmic losses, copper linac can be efficiently used only in low-gradient, cw operations or high-gradient, pulsed operations. The accelerators and supporting RF equipment (e.g., klystrons, power supply) are often the largest components of the normal-conducting linac FEL. For true cw operation, normal-conducting copper linac are inferior to SRF linac mainly because SRF linac offer higher cw accelerating gradients at much lower ohmic losses, by virtue of much higher electrical conductivity of the superconducting surfaces. SRF linac technology can potentially lead to a more compact design of cw accelerators. However, the niobium cavities have to be cooled to 2 K. Since the thermodynamic efficiency of heat removal is lower at cryogenic temperatures, a large helium cryoplant is required to cool the SRF cavities. In addition, SRF cavities have to be designed to operate at high average current, at the same time minimizing the risk of beam breakup instabilities (BBU). Regenerative BBU in same-cell energy recovery sets a limit on the average current that can be accelerated through the SRF cavities.[1]

A key development in recent years is the large exponential gains that result from the use of a high-brightness (high-peak-current, low-emittance, low-energy-spread) electron beams.[7] Large single-pass gains in self-amplified spontaneous emission (SASE) FELs have been observed at wavelengths ranging from millimeters to vacuum UV.[8] Efforts are underway to build a SASE x-ray FEL at the Stanford Linear Accelerator Center. We foresee that the large single-pass gains will also enable a large increase in the micropulse energy, from the microjoule level of the oscillator FEL to a few millijoules of the amplifier FEL. The large single-pass gain enables 100% out-coupling fraction—in the absence of damage-prone and vibration-sensitive resonator mirrors—and high wiggler extraction efficiency.

Uniform wiggler section Tapered wiggler section

Fig. 3. Combination wiggler configuration with uniform and tapered wiggler sections.

The FEL extraction efficiency can be enhanced with the use of a combination wiggler, one with both uniform and tapered sections (Fig. 3). The uniform section provides the exponential gain to amplify a low-intensity input signal to near saturation. The electrons in the original energy distribution interact with the growing optical field and rotate in the expanding ponderomotive bucket (shown in red) by one-quarter of the synchrotron period. The tapered section then provides efficient energy extraction from the prebunched electron beam by trapping and decelerating about 50% of the electrons in a decelerating bucket. As the bucket moves down in energy, the trapped electrons oscillate inside it and give up more power to the optical field. The electron energy distribution will contain two peaks, one at the original energy and the other at the centroid of the decelerated bucket.

The energy of the electron beams exiting the wiggler can be recovered to improve overall electrical efficiency and to reduce radiation hazard. In principle, high average power and efficiency can be achieved with a properly tapered wiggler and energy recovery of the spent electron beams. However, practical considerations in transporting electron beams with a large energy spread in the bends and decelerators for energy recovery have hitherto precluded high-efficiency wigglers. In this paper, we suggest the use of energy-spread compression to recirculate the electron beams exiting a tapered wiggler. We show with simulations that a 3.5% efficient tapered wiggler will produce 10% energy spread in the electron beam. Such an electron beam can be transported around a large-energy-acceptance bend to separate energy recovering decelerating linac.

2. Amplifier FEL Basics

The output wavelength of an FEL is determined by the wiggler period, the wiggler magnetic field, and the electron beam energy as given by the FEL resonance condition

$$\lambda = \frac{\lambda_w}{2\gamma^2}\left(1 + a_w^2\right) \tag{1}$$

where the symbols are defined in Table I.

In the exponential gain regime, the optical power of an FEL amplifier starts from P_0 at $z = 0$ (the wiggler entrance) and grows exponentially with z, the distance in the wiggler until it saturates at the maximum power P_{max}[3]:

$$P(z) = \frac{1}{9}\frac{P_0 e^{z/L_G}}{\left[1 + \frac{1}{9}(P_0/P_{max})(e^{z/L_G} - 1)\right]} \tag{2}$$

The saturation power P_{max} is given by $P_{max} \approx \rho P_b$ for a uniform wiggler and $P_{max} \approx (\Delta\gamma/\gamma_0)\eta_C P_b$ for a tapered wiggler, where ρ the Pierce parameter is defined for a

Table 1. Commonly used FEL symbols, their definitions, and design values for a 1-μm FEL amplifier

Symbol	Definition	Design value
λ	FEL wavelength	1.06 μm
λ_w	Wiggler period	2.18 cm
a_w	Wiggler dimensionless parameter	1.085
L_w	Uniform wiggler length	9 m[a]
B_w	Uniform wiggler magnetic field	0.75 T
$\Delta\gamma/\gamma_0$	Wiggler energy taper	7.5%
L_{taper}	Tapered wiggler length	6 m
f_B	Difference in Bessel functions for the above planar wiggler	0.848
E_b	Electron beam energy	76 MeV
γ	Electron beam Lorenz factor	150
I	Electron beam peak current	400 A
P_b	Electron beam peak power ($I \cdot E_b$)	30.4 GW
I_A	Characteristic current	17 kA
q	Electron bunch charge	3 nC
τ	Electron bunch length	8 ps
ε_n	Electron beam emittance	15 μm
σ_γ	Electron beam energy spread	0.25% rms
β	Electron focusing beta function	0.68 m
σ	Electron beam radius (rms)	370 μm
ρ	FEL gain parameter	0.01
L_G	3D FEL power gain length	37 cm
Λ_{3D}	3D gain reduction factor	0.5
P_0	Input optical power	0.1 W
P_{peak}	Peak FEL power	1.05 GW
η_C	Electron capture efficiency	50%
η_{FEL}	FEL extraction efficiency	3.5%
w_0	FEL beam 1/e^2 radius	0.53 mm
θ	FEL beam divergence half-angle	0.3 mrad

[a]This uniform wiggler length is needed if the input laser power is only 0.1 W (incoherent noise). The uniform wiggler length can be shortened considerably if an actual input laser beam is injected into the amplifier. For example, an input power of 20-kW peak (about 20-W average power) will shorten the required wiggler length to 4 m.

planar wiggler as follows:

$$\rho = \left(\frac{a_w \lambda_w f_B}{4\pi\gamma}\right)^{2/3} \left(\frac{I}{2 I_A \beta \varepsilon_n}\right)^{1/3} \tag{3}$$

Note that the Pierce parameter is both an exponential gain factor and a saturated efficiency for a high-gain FEL. It is therefore important to maximize ρ for both gain and efficiency. The exponential gain length, the length over which the optical power grows by one e-fold, is denoted L_G. This power gain length, in addition to being inversely proportional to ρ, depends on three-dimensional (3D) effects such as diffraction, emittance, and energy spread. The power gain length can be calculated using the variational approximation[10]

$$L_G = \frac{\lambda_w}{4\pi\sqrt{3}\rho}(1 + \Lambda_{3D}) \tag{4}$$

To achieve high gains in a reasonable wiggler length, one minimizes the gain length by employing high-peak-current (increasing-ρ), low-emittance, low-energy-spread electron beams. (The latter minimize the 3D gain-reduction term Λ_{3D}.)

In a SASE FEL, the optical power reaches saturation when the electrons rotate one-half of the synchrotron period in longitudinal phase-space. The saturated efficiency of a SASE FEL with uniform wigglers is given approximately by $\rho/(1 + \Lambda_{3D})^2$. Since ρ, the FEL gain parameter, is typically 1–2%, the saturated SASE efficiencies with a uniform wiggler are less than 1%. Slippage, an effect whereby the optical pulses move ahead of the electron bunches, in the long wiggler further reduces the wiggler efficiency. To improve FEL extraction efficiency, one must use a tapered wiggler in addition to the high-gain uniform wiggler to maintain the resonance condition as the electron beams lose energy. For a linear taper, i.e., the wiggler period or magnetic field decreases linearly with length, the tapered wiggler efficiency is given by the wiggler's energy taper and the capture efficiency η_C, which is a function of the FEL intensity and the taper rate. The energy taper is accomplished either by tapering the wiggler period or the magnetic field:

$$\frac{\Delta\gamma}{\gamma_0} = \frac{\Delta\lambda_w}{2\lambda_w} + \frac{a_w^2}{1 + a_w^2}\frac{\Delta B_w}{B_w} \tag{5}$$

As an example, if the period is kept constant and a_w, the rms wiggler parameter at the entrance of tapered section, is unity, the energy taper for a 15% magnetic field taper is 7.5% of the initial energy. The tapered wiggler efficiency is a function of the energy taper, the FEL optical intensity, and the taper rate:

$$\eta_{\text{taper}} = -\frac{\Delta\gamma}{\gamma_0} \cdot \eta_C\left(I, \frac{\Delta\gamma}{\gamma_0 L_{\text{taper}}}\right) \tag{6}$$

If the 7.5% energy taper is linear over 6 m, corresponding to a magnetic field taper rate of 2.5%/m, the calculated capture efficiency will be about 50% for an optical intensity of 7.5 GW/cm^2 at the tapered wiggler entrance, giving rise to an FEL extraction efficiency of 3.7%. This efficiency can be improved by using a longer tapered wiggler at a constant taper rate or the same tapered wiggler length at a larger taper rate and a higher optical intensity. For instance, if a 15% energy-taper wiggler is used with 12 m of tapered wiggler, the FEL extraction efficiency will be as high as 8%. The long wiggler will require a longer micropulse ($>$10 ps) to minimize slippage, which is also desirable as this will lead to higher micropulse energy. The high wiggler efficiency reduces the required electron beam power, thus lowering the required beam energy (fewer linac modules) or current (minimizing BBU risks).

The optical beam of an FEL amplifier is not defined by an optical resonator but by optical guiding, i.e., the optical beam's transverse profile follows the electron beam's profile inside the high-gain uniform wiggler. The rms radius of the FEL beam is determined by the electron beam's emittance, the electron focusing optics β function. Inside the tapered wiggler, optical guiding decreases sharply and the FEL beam expands at a rate approximately inversely proportional to the electron beam radius. The FEL beam expansion inside the tapered wiggler can be used to decrease the beam intensity below the damage threshold of any optics downstream from the wiggler.

3. Amplifier FEL with Energy Recovery

A possible configuration of the high-power, high-gain FEL amplifier with energy recovery is shown in Fig. 4. The electron beam travels counterclockwise, starting from the injector on the right (middle row), going around the ring one and a half times, and terminating at the beam dump. The FEL beam exiting the wiggler passes through the linac at the lower-right-hand corner of the ring.

An RF injector is used to produce the electron beam with the requisite peak current, beam emittance, and energy spread. The electron beam is accelerated in a number of linac modules slightly off-crest of the RF field to introduce an energy chirp along the bunch. At an intermediate energy (sufficiently high to minimize space charge effects), the electron beam turns around in an achromatic and isochronous 180-deg bend. A magnetic chicane immediately after the 180-deg bend compresses the chirped electron beam to the desired bunch length but still preserves part of the energy chirp (undercompression). Electron bunch compression is done after the 180-deg bend to minimize coherent synchrotron radiation effects caused by short electron bunches going in circular arcs. Owing to second-order curvatures of the RF field and the chicane compressor, the partially compressed electron bunch will have nonlinearity in its energy-phase distribution.[2] The chirped beam then traverses two more linac and comes to complete bunching at the wiggler entrance. Single-bunch beam loading (wakefields) in the linac corrects for the nonlinearity in the chirped bunch and reduces the beam's energy spread. The bunched beam is then injected into a wiggler with two-plane (weak) or strong focusing. The input signal for the amplifier comes from an external laser shown on the left. The uniform wiggler length is chosen so that the electrons rotate one-quarter of the synchrotron period before the taper begins. The FEL beam inside the tapered wiggler (with the wiggler field tapered shown as increasing wiggler gap) extracts energy from the prebunched electron beams.

To increase wall-plug efficiency, energy recovery should be used in combination with the tapered wiggler. The spent electron beam from the tapered wiggler returns to the energy recovery decelerators in a large-energy-acceptance, 180-deg bend. To transport most of the electron beam to the beam dump, one needs to compress the electron beam's energy spread with a chicane–linac momentum compactor. The 180-deg bend will be designed to

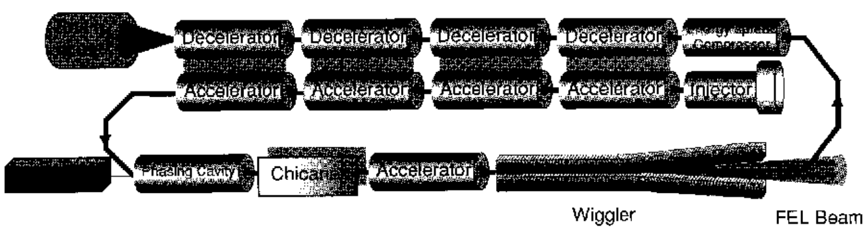

Fig. 4. Schematic of the high-power, high-gain amplifier FEL with energy recovery.

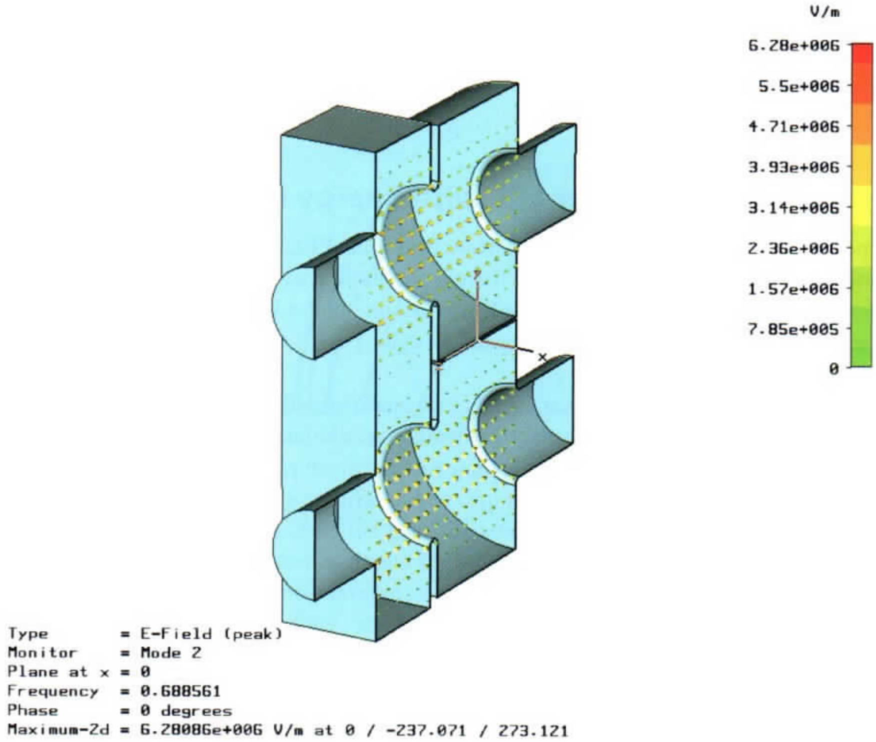

Fig. 5. Possible configuration of an energy recovery system consisting of two SRF cavities, one as an accelerating cavity and the other a decelerating one, connected via a waveguide.

have dispersion and will rotate the electron beam's longitudinal phase-space. The beam then traverses a linac operating off crest at the decelerating phase so that electrons at the initial energy lose energy faster the lower energy electrons (those that lose energy in the wiggler). The energy spread is thus compressed at the expense of an increase in bunch length. The decelerating cavities further rotate the longitudinal phase-space ellipse, recover approximately 60 MeV of the electron beam energy, and thus reduce the beam energy to about 10 MeV or less. The recovered RF power flows back into the accelerating cell via a superconducting waveguide between the decelerating and accelerating cells (Fig. 5). Both accelerating and decelerating cavities and the waveguide can be packaged inside one common cryostat.

4. Simulations

Simulations were performed to test the feasibility of a high-gain FEL amplifier operating at 1.06 μm. The 76-MeV beam energy is chosen as this saves linac length and RF power. If the normalized emittance at the wiggler entrance is not sufficiently low, it may be necessary to increase the beam energy further. Table I lists the parameters for MEDUSA and PARMELA simulations.

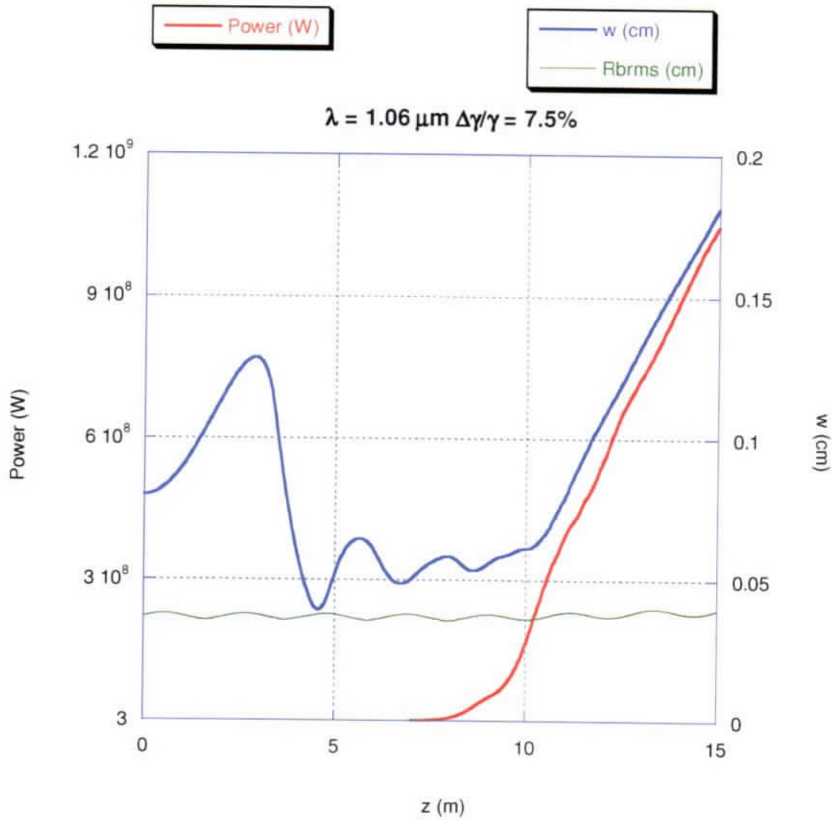

Fig. 6. MEDUSA simulations of FEL power (red), optical mode radius (blue), and electron rms radius (green) vs distance. The uniform wiggler extends from 0 to 9 m and the tapered from 9 to 15 m. The optical mode is trapped in the uniform wiggler and expands at a constant rate in the tapered wiggler.

We use the 3D, polychromatic FEL simulation code MEDUSA.[4] MEDUSA can model planar and helical wiggler geometries and treats the electromagnetic field as a superposition of either Gauss–Hermite or Gauss–Laguerre modes. The field equations are integrated simultaneously with the 3D Lorentz force equations. No wiggler-average orbit approximation is used, and MEDUSA propagates the electrons through a complex wiggler/transport line including multiple wiggler sections, tapered wigglers, quadrupole and dipole corrector magnets, focusing-drift-defocus-drift (FODO) lattices, and magnetic chicanes.

Figure 6 shows the power growth curve for a combination wiggler consisting of a 9-m uniform section and a 6-m tapered section. The uniform wiggler increases the optical power from 0.1 W to 50 MW, below the saturation level of 300 MW. The tapered wiggler increases the peak FEL power from 50 MW to 1.05 GW. The wiggler length can be shortened considerably if the "seed" power is much greater than 0.1 W. The electron beams exiting the tapered wiggler acquire a bimodal energy distribution (Fig. 7), one at the original energy of 76 MeV and the other at the decelerated energy of 70.6 MeV (7% reduction in energy from 76 MeV).

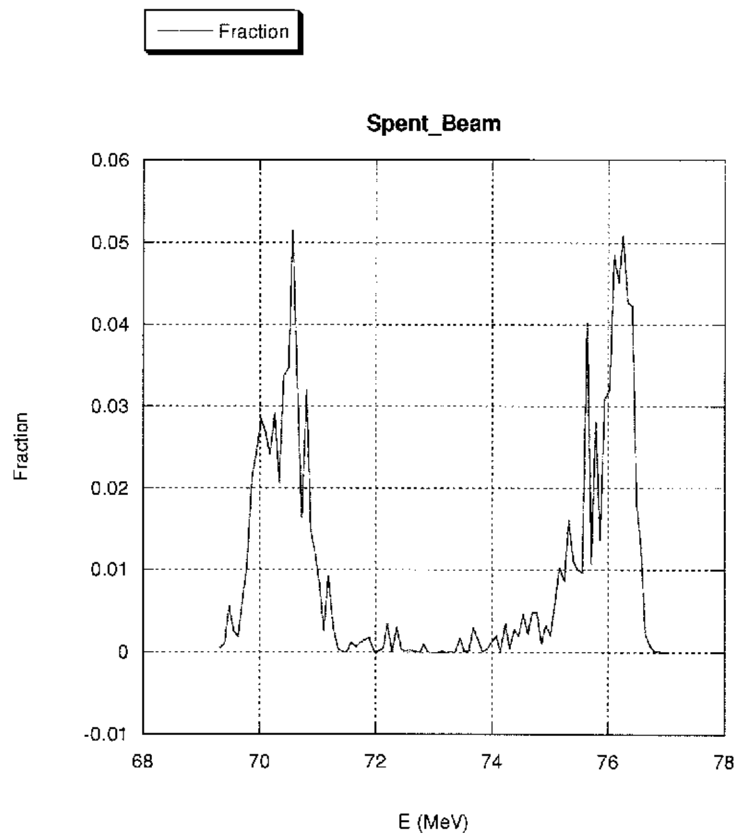

Fig. 7. MEDUSA simulation of the spent electron beam energy distribution.

5. Conclusions

We have outlined a possible approach to high-power FEL using recent advances in high-brightness electron beam generation and high-gain FEL amplifier. Using conservative beam parameters that can be achieved with today's high-brightness beam generation and nonlinear bunch compression, the amplifier FEL can produce 1-GW peak power external to the FEL and 8 mJ of micropulse energy. We expect with optimization the tapered wiggler extraction efficiency could be increased to the 10% level. The optical pulses can also be chirped (by imposing an energy slew on the electron beam) and then compressed by propagating in the atmosphere to achieve even higher peak power on a distant target. High average power can be achieved by operating the FEL amplifier at high duty factor, e.g., high micropulse repetition rate. The FEL amplifier can potentially produce high power without the problem of optical damage to the mirrors of the high-Q optical resonator. Energy recovery is also possible with a tapered wiggler if a large-energy-acceptance, 180-deg bend is used to transport the spent beam and if the proposed energy compression technique is effective in reducing the spent beam's energy spread. A possible configuration for energy recovery in separate decelerating structures has been shown, with RF power coupled back to the accelerating structures via resonant bridge couplers.

6. Acknowledgments

We appreciate the financial support from the Department of Defense High-Energy Laser Joint Technology Office via a contract by NAVSEA. We also thank Bruce Carlsten, Steven Russell, and James Potter for helpful discussions.

References

[1]Bisognano, J.J., and R.L. Gluckstern, *1987 Particle Accelerator Conference*, p. 1078 (1987).

[2]Carlsten, B.E., Nucl. Instr. Meth. Phys. Res. A **380**, 505 (1996).

[3]Dattoli, G., L. Giannessi, P.L. Ottaviani, and M. Carpanese, Nucl. Instr. Meth. Phys. Res. A **393**, 133 (1997).

[4]Freund, H.P., S.G. Biedron, and S.V. Milton, IEEE J. Quantum Electron. **36**, 275 (2000).

[5]Neil, G.R., S. Benson, G. Biallas, C.L. Bohn, D. Douglas, H.F. Dylla, R. Evans, J. Fugitt, A. Grippo, J. Gubeli, R. Hill, K. Jordan, R. Li, L. Merminga, P. Piot, J. Preble, M. Shinn, T. Siggins, R. Walker, and B. Yunn, Phys. Rev. Lett. **84**, 662 (2000).

[6]Nguyen, D.C., L.M. Earley, N.A. Ebrahim, C.M. Fortgang, J.C. Goldstein, R.F. Harrison, W.A. Reass, J.M. Kinross-Wright, R.L. Sheffield, and S.K. Volz, *Proceedings of the XX International Linac Conference*, p. 731 (2000).

[7]Nguyen, D.C., R.L. Sheffield, C.M. Fortgang, J.C. Goldstein, J.M. Kinross-Wright, and N.A. Ebrahim, Phys. Rev. Lett. **81**, 810 (1998).

[8]O'Shea, P., and H. P. Freund, Science, **292**, 1853 (2001).

[9]Urbanus, W.H., W.A. Bongers, C.A.J. vanderGeer, P. Manintveld, J. Plomp, J. Pluygers, A.J. Poelman, P.H.M. Smeets, F.C. Schuller, and A.G.A. Verhoeven, Nucl. Instr. Meth. Phys. Res. A **429**, 12 (1999).

[10]Xie, M., Nucl. Instr. Meth. Phys. Res. A **445**, 59 (2000).